Model Simulations Examining the Relationship of Lake-Effect Morphology to Lake Shape, Wind Direction, and Wind Speed

NEIL F. LAIRD AND JOHN E. WALSH

Department of Atmospheric Sciences, University of Illinois at Urbana–Champaign, Urbana, Illinois

DAVID A. R. KRISTOVICH

Atmospheric Environment Section, Illinois State Water Survey, Illinois Department of Natural Resources, Champaign, and University of Illinois at Urbana–Champaign, Urbana, Illinois

(Manuscript received 3 December 2002, in final form 20 March 2003)

ABSTRACT

Idealized model simulations with an isolated elliptical lake and prescribed winter lake-effect environmental conditions were used to examine the influences of lake shape, wind speed, and wind direction on the mesoscale morphology. This study presents the first systematic examination of variations in lake shape and the interplay between these three parameters. The array of 21 model simulations produced cases containing each of the three classic lake-effect morphologies (i.e., vortices, shoreline bands, and widespread coverage), and, in some instances, the mesoscale circulations were composed of coexisting morphologies located over the lake, near the downwind shoreline, or inland from the downwind shore.

As with lake-effect circulations simulated over circular lakes, the ratio of wind speed (U) to maximum fetch distance (L) was found to be a valuable parameter for determining the morphology of a lake-effect circulation when variations of lake shape, wind speed, and wind direction were introduced. For a given elliptical lake and strong winds, a morphological transform from shoreline band toward widespread coverage accompanied changes in ambient flow direction from along to across the major lake axis. For simulations with weak winds over a lake with a large axis ratio, the morphology of the lake-effect circulation changed from vortex toward shoreline band with a change in wind direction from along to across the major lake axis. Weak winds across lakes with smaller axis ratios (i.e., 1:1 or 3:1) produced mesoscale vortices for each wind direction. Across the array of simulations, a shift in mesoscale lake-effect morphology from vortices to bands and bands toward widespread coverage was attended by an increase in U/L. Last, the elliptical-lake results suggest that the widths of the lake-effect morphological transition zones in U/L parameter space, conditions favorable for the coexistence of multiple morphologies, were greater than for circular lakes.

1. Introduction and background

Lake-effect (LE) meso-β-scale circulations (i.e., 20–200 km) that develop as a result of cold arctic air moving over an individual lake can produce severe winter weather for nearshore communities in the Great Lakes region (or other locations that experience LE, such as the Great Salt Lake). These mesoscale systems can often produce significant snow accumulations within very short time periods, which may negatively impact transportation systems, limit business operations, and cause significant property damage. These LE mesoscale circulations are often characterized by a distinct morphology (Braham and Kelly 1982; Hjelmfelt 1990; Niziol et al. 1995). The four most commonly discussed morphologies include 1) widespread coverage (e.g., Kelly 1986; Kristovich and Laird 1998), 2) shoreline bands (e.g., Hjelmfelt and Braham 1983), 3) midlake bands (e.g., Passarelli and Braham 1981), and 4) mesoscale vortices (e.g., Forbes and Merritt 1984; Laird 1999). For this study, shoreline and midlake bands are consolidated into a single morphological regime called "shoreline bands" since lower-tropospheric convergence from spatial variations in frictional drag and surface diabatic forcing, frequently used to distinguish these two types of LE bands, occur simultaneously (Holroyd 1971).

Although mesoscale LE circulations develop through complex interactions of an array of environmental and geographic variables (e.g., lake–air temperature difference, wind speed, lower-tropospheric stability, lake shape), it is well established that the distribution of the surface thermal gradient (e.g., shoreline configuration) and interaction with the ambient wind may enhance or diminish the low-level convergence and the vertical circulation (e.g., McPherson 1970). For example, Rothrock

Corresponding author address: Neil F. Laird, Dept. of Atmospheric Sciences, University of Illinois at Urbana–Champaign, 105 South Gregory St., Urbana, IL 61801.
E-mail: n-laird@uiuc.edu

(1969) and Holroyd (1971) observed that long, relatively narrow lakes, such as Lakes Michigan, Erie, and Ontario, generally have a narrow range of wind directions that may be favorable for significant lake snow events, while broader lakes with more irregular shorelines, such as Lakes Superior and Huron, may produce heavy snows over a larger range of wind directions.

Laird et al. (2003) conducted a study using a series of idealized mesoscale model simulations of LE conditions over an isolated circular lake to examine the influence of varied conditions (i.e., wind speed, lake–air temperature difference, ambient atmospheric stability, and fetch distance) on LE morphology. They found that the ratio of wind speed (U) to maximum fetch distance (L) effectively indicated the meso-β-scale LE morphology. The ratio U/L is equivalent to the inverse advective residence time of an air parcel over a lake, and its relationship with LE morphology was found to be independent of the lake–air temperature difference (ΔT) for events with $\Delta T > 5°C$. Lake-effect environmental conditions producing low values of U/L (i.e., <0.02 m s^{-1} km^{-1}) resulted in a mesoscale vortex. Conditions leading to U/L values between about 0.02 and 0.09 m s^{-1} km^{-1} resulted in the development of a shoreline band, and U/L values greater than approximately 0.09 m s^{-1} km^{-1} produced a morphology of widespread coverage. Additionally, Laird et al. (2003) found that transitions from one morphological regime to another in U/L parameter space were continuous, and within transitional zones the structure of a circulation may contain features characteristic of two LE morphologies. Similarly, observations presented by Pitts et al. (1977), Schoenberger (1986), and Laird (1999) indicate the occurrence of events where multiple LE morphologies (e.g., mesoscale vortices and shoreline band) coexisted over a single lake.

Since L varies with wind direction for noncircular lakes, it is anticipated that variations in lake shape, wind direction, and wind speed influence the resulting meso-β-scale morphology of LE circulations and the location of heaviest snowfall. While past studies have discussed the influence of wind direction and wind speed on LE intensity and morphology for a specific lake, such as Lake Erie (e.g., Lavoie 1972; Niziol 1987) or Lake Michigan (e.g., Hsu 1987; Hjelmfelt 1990), the effects of variations in lake shape are more difficult to address and have not been systematically examined. The current investigation, a companion study to Laird et al. (2003), uses idealized mesoscale model simulations to examine the influence of variations in lake shape, wind direction, and wind speed on the morphology of LE mesoscale circulations. The mesoscale model and simulated conditions used for the current study are discussed in section 2. Section 3 presents the results of the investigation, and section 4 summarizes the findings.

2. Mesoscale model and model setup

The Colorado State University Mesoscale Model (CSUMM) used for this investigation is a three-dimensional, hydrostatic, incompressible, primitive equation model originally developed by Pielke (1974) to study the Florida sea-breeze circulation. The CSUMM has been modified and enhanced over the past several decades and has been used to successfully simulate LE snowstorms (e.g., Hjelmfelt and Braham 1983; Pease et al. 1988; Hjelmfelt 1990; Laird et al. 2003). Only a brief discussion of the model is provided; however, a complete description of the model version used for this study is contained in Laird (2001), and specification of the simplified model physics is provided in Laird et al. (2003).

The CSUMM requires terrain information (topographic elevations, water/land coverage) and initial vertical profiles of temperature, specific humidity, and wind. The initial wind profile is used to establish both the uniform geostrophic wind and the initial horizontally uniform actual wind profile. Zero-gradient lateral-boundary conditions were assumed for all prognostic variables. In addition, the lateral boundaries were far removed from the region of interest to avoid contamination of the model solution by boundary effects. At the lower boundary, a no-slip condition was specified for the horizontal velocities ($u = v = 0$) and the vertical velocity was $w = 0$. A constant value for the Coriolis parameter [$f = 2\Omega \sin(44°$ latitude), where $\Omega = 7.292 \times 10^{-5}$ s^{-1}] was used throughout the entire domain. This simplification allowed a smaller array of simulations to be conducted and the elliptical lake to be oriented with the major axis in the north–south direction for all simulations. Several preliminary simulations showed that under the same atmospheric conditions the resulting LE circulations were identical for an elliptical north–south- or east–west-oriented lake, suggesting that the results from this study are applicable to all lake orientations.

For this study, atmospheric water vapor was considered a passive scalar quantity that could be advected by the wind, diffused by turbulence, and exchanged at the surface. In an effort to reduce large computational time and model output storage capacity for the model simulations performed, latent heating and precipitation processes were not included. The exclusion of these processes should not have a major influence on the qualitative results of this study since previous LE investigations (e.g., Hjelmfelt 1990; Cooper et al. 2000) have shown that although the strength of the lake-induced circulations may be reduced, the structure is maintained in the absence of moist microphysical processes and associated latent heating. In addition, solar radiation calculations were not included in the simulations.

Twenty-one model simulations were conducted using an isolated elliptical lake and horizontal grid spacing of 10 km. Flat topography was used and 20 model levels were included, with separation of levels increasing with height. Environmental conditions included wind directions from the west, northwest, or north; lake axis ratios of 1:1, 3:1, or 9:1; and wind speeds of 1.0, 10.0, or 18.2 m s^{-1}. These values of axis ratio span those of lakes within the Great Lakes region. The lengths of the major axis and minor axis of the 3:1 elliptical lake were 350 and 114 km, respectively. The lengths of the major axis and minor axis of the 9:1 elliptical lake were 600 and 66 km, respectively. For comparison, the lake axis ratios of Lakes Superior, Huron, Michigan, Erie, and Ontario are approximately 2:1, 1:1, 3:1, 4:1, and 4:1, respectively.

To allow each simulation to be initialized with a consistent surface heat source, the elliptical lakes had an equivalent surface area of approximately 31 400 km^2 (equivalent to a 200-km circular lake) and a ΔT (the difference between the lake surface and upwind 10-m air temperatures) of 22.5°C. A constant, uniform lake surface water temperature of 0°C was prescribed. A constant initial stability existed from the surface to 1.5 km ($d\theta/dz$ = 1.0 K km^{-1}). From 1.5 to 3.5 km, a stable layer was prescribed as a smooth transition to $d\theta/dz$ = 8.0 K km^{-1} above 3.5 km. Similar profiles have often been observed upwind of lakes during LE events (e.g., Hjelmfelt and Braham 1983; Laird 1999) and used in prior idealized LE modeling investigations (e.g., Hjelmfelt 1990; Sousounis 1993; Rose 2000). Wind profiles were prescribed using a uniform speed and direction throughout the entire profile. The model initialization included a modified-Ekman-balanced boundary layer in order to incorporate surface friction into the initial wind field. The specification of the idealized atmospheric environment was based on typical conditions observed during Arctic cold-air outbreaks and previously observed LE conditions in the Great Lakes region (e.g., Braham and Kelly 1982). In addition, conditions found to be favorable for the development of vortex, shoreline band, and widespread coverage morphologies in the idealized circular-lake LE simulations from Laird et al. (2003) were used to help select the conditions for the current study.

A 36-h simulation was performed for each experiment using a time step of 40 s. This allowed the initially uniform conditions to respond to the positive (i.e., surface to atmosphere) heat fluxes associated with the lake and inhomogeneous surface friction. By 24 h, the time period for which the results are presented, the LE circulation had generally reached maximum intensity and a quasi-steady circulation was sustained in each simulation (Laird et al. 2003).

3. Results

Results from Laird et al. (2003) showed that the quantity U/L was a useful indicator for determining the LE morphology for circular lakes. In the current study, we use idealized model simulations with elliptical lakes to examine this relationship further when variations in lake shape, wind direction, and wind speed are introduced. The criteria used to differentiate the meso-β-scale LE structures are similar to those used by Laird et al. (2003) and are primarily based on the examination of near-surface wind fields for characteristic features associated with different LE morphologies. A mesoscale vortex was identified when a closed cyclonic circulation was exhibited in the low-level wind field over the lake. The presence of a land-breeze wind component confined near the downwind shore and a line of convergence over the lake was used to identify the shoreline band morphology. This definition is consistent with both observations of intense LE band events (e.g., Passarelli and Braham 1981; Braham 1983; Schoenberger 1986) and the definition used by Hjelmfelt (1990) when examining simulated shoreline bands. A morphology of widespread coverage was identified when the flow across the lake was nearly unidirectional and the downwind-shore land breeze was not present, even though weak low-level convergence often remained over this area. In this section, we present 1) output from several model simulations to examine and compare the resulting mesoscale LE morphology for 3:1 and 9:1 axis ratio experiments and 2) the performance of U/L as an indicator of LE morphology using the 21 model simulations with an elliptical lake.

a. Model output fields

Figures 1–3 present the surface pressure, 10-m horizontal wind, and 1500-m vertical motion fields for lakes with 3:1 and 9:1 axis ratios. Model output fields over both the 3:1 and 9:1 lakes are shown for vortex (Fig. 1), shoreline band (Fig. 2), and widespread coverage (Fig. 3) morphologies that occurred with northwest ambient flows of 1.0, 10.0, and 18.2 m s^{-1}, respectively. Several of these simulations also provide examples of coexisting LE morphologies (Figs. 1c,d; 2c,d; 3a,b). The differences and similarities in mesoscale structure and a comparison to results from simulations with circular lakes (Laird et al. 2003) are highlighted below. Results from simulations with westerly and northerly winds were similar to those presented, although the LE morphology of north and west wind simulations tended to result in shoreline band and widespread coverage morphologies, respectively. This result will be discussed further in section 3b. A summary for all 21 simulations included in this study and their U/L values is given in the appendix.

1) 1.0 M S^{-1} NORTHWEST WIND SIMULATIONS

Figures 1a,b show model fields produced for a northwest flow of 1.0 m s^{-1} over an elliptical lake having a 3:1 axis ratio. A meso-β-scale vortex develops, similar to simulations with circular lakes and an equivalent U, ΔT, and N (see Figs. 3a,b of Laird et al. 2003); however, the vortex is elongated along the major lake axis. The reduction in frictional drag of the upwind offshore flow and the land breeze due to the development of the mesoscale low-pressure center (hereafter referred to as the mesolow) over the lake, enhanced the northwesterly flow along the western lakeshore. The land-breeze flow along the eastern shoreline was slightly weaker because

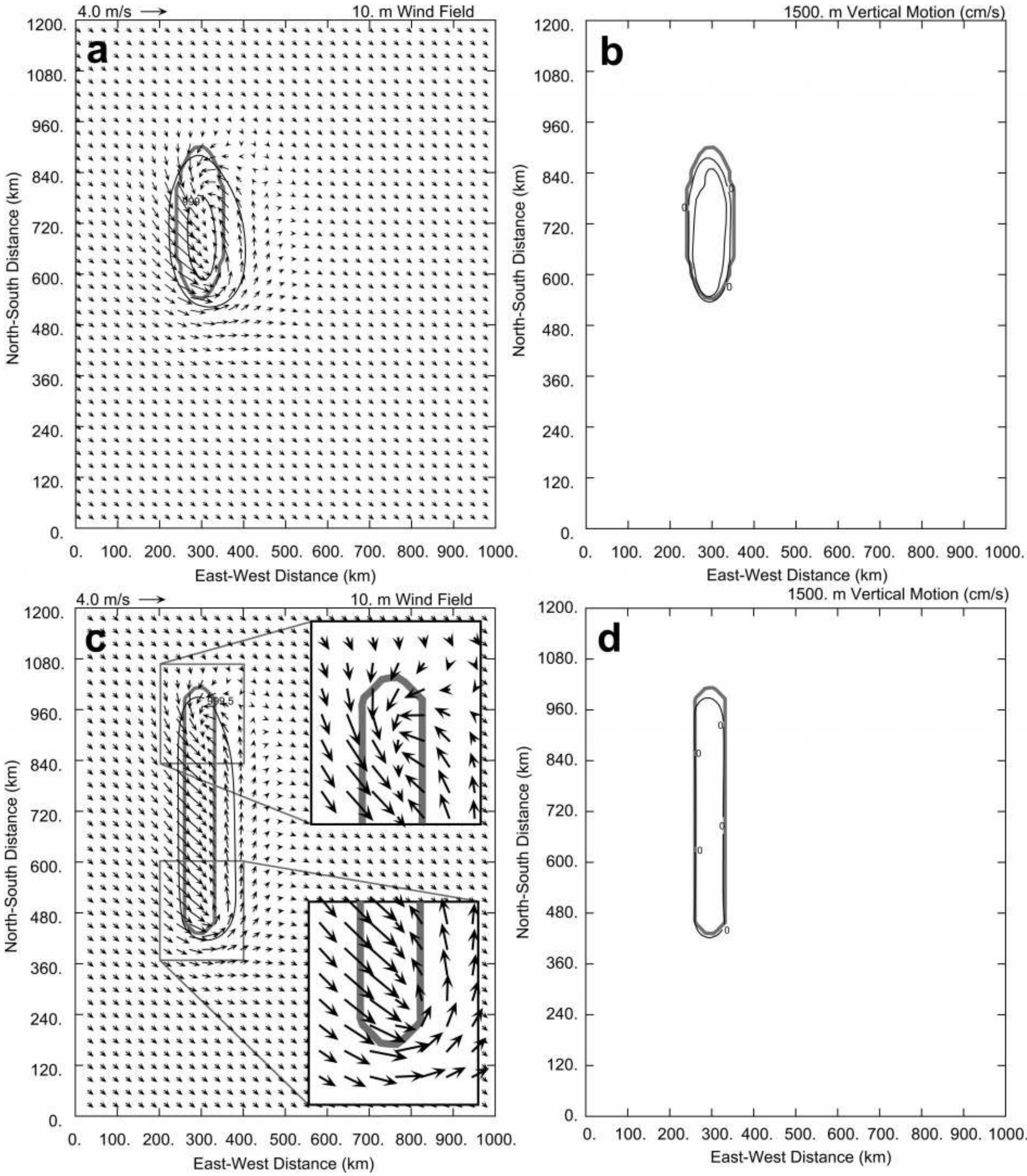

FIG. 1. The (left column) 10-m wind, surface pressure, and (right column) 1500-m vertical motion fields for (a), (b) a 3:1 axis ratio lake and (c), (d) a 9:1 axis ratio lake with an ambient wind speed of 1.0 m s^{-1} from the northwest. Surface pressure and vertical motion fields have contour intervals of 0.5 hPa and 5.0 cm s^{-1}, respectively.

of the thermal modification of the atmosphere downwind of the lake and the reduction of the surface pressure gradient over the downwind region (Fig. 1a). The updraft associated with the vortex was confined to the overlake region with a maximum of approximately 5.0 cm s^{-1}, which was nearly equivalent to updrafts produced for the corresponding simulation with a circular lake.

Figures 1c,d show model fields simulated for a northwest flow of 1.0 m s^{-1} over an elliptical lake with a 9:1 axis ratio. The structure of the circulation has attributes of both a shoreline band and vortex. Mesoscale

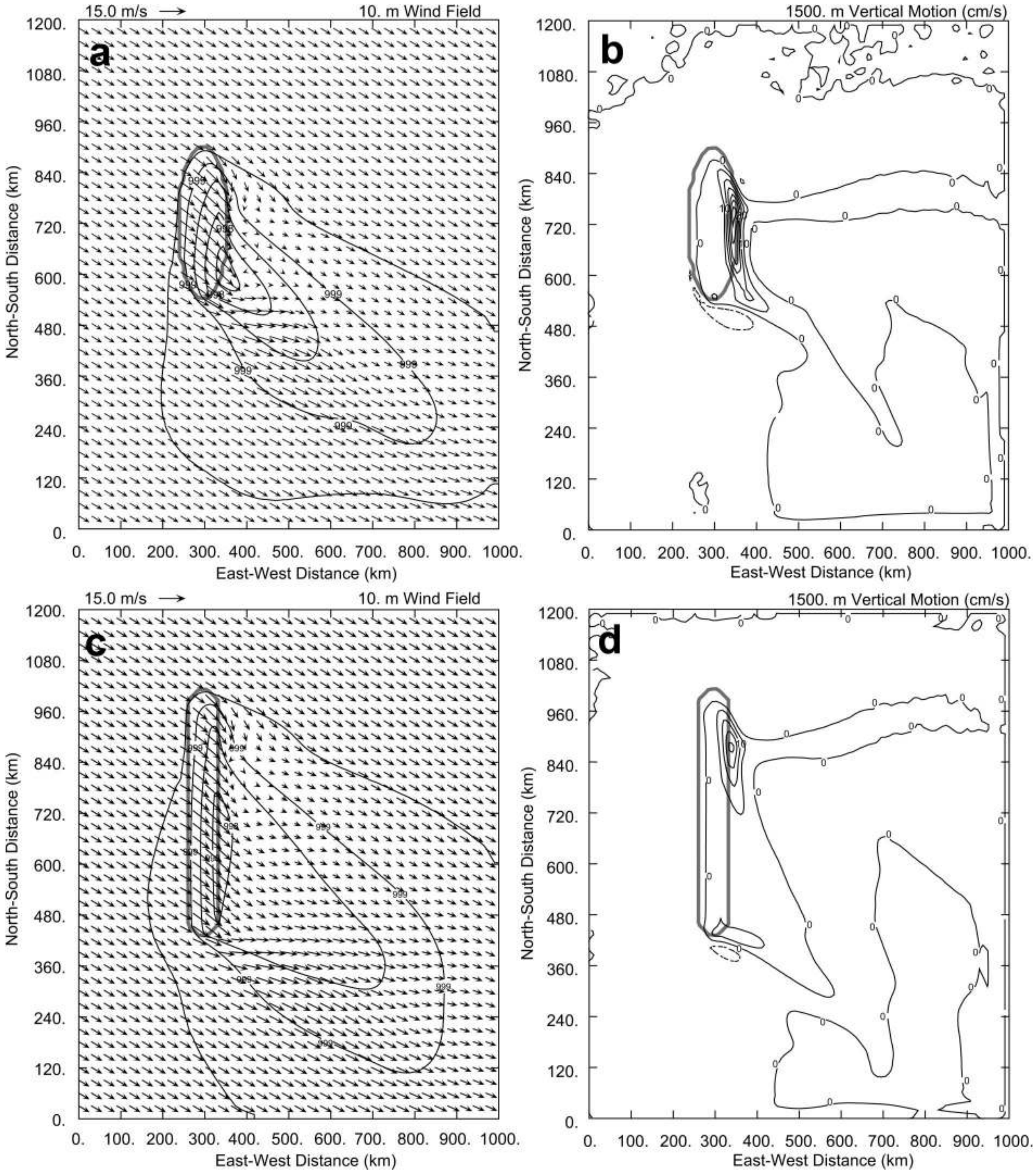

FIG. 2. Same as Fig. 1, but with an ambient wind speed of 10 m s^{-1}.

cyclonic vortex circulations are present over the northern and southern regions of the lake. Both the mesolow and the overlake updraft are slightly weaker than those produced in the 3:1 lake axis ratio simulation (Figs. 1a,b). A north–south zone of low-level convergence resulting from the interaction of the western- and eastern-shore land breezes extends nearly the entire length of the lake. The combined band and vortex structures are similar to observations presented by Laird (1999) of a multiple LE vortex event over the western Great Lakes and model results of Hjelmfelt (1990) and Pease et al. (1988).

2) 10.0 M S^{-1} NORTHWEST WIND SIMULATIONS

Figures 2a–d show model fields for the 3:1 and 9:1 simulations with a northwest wind of 10 m s^{-1}. Figures

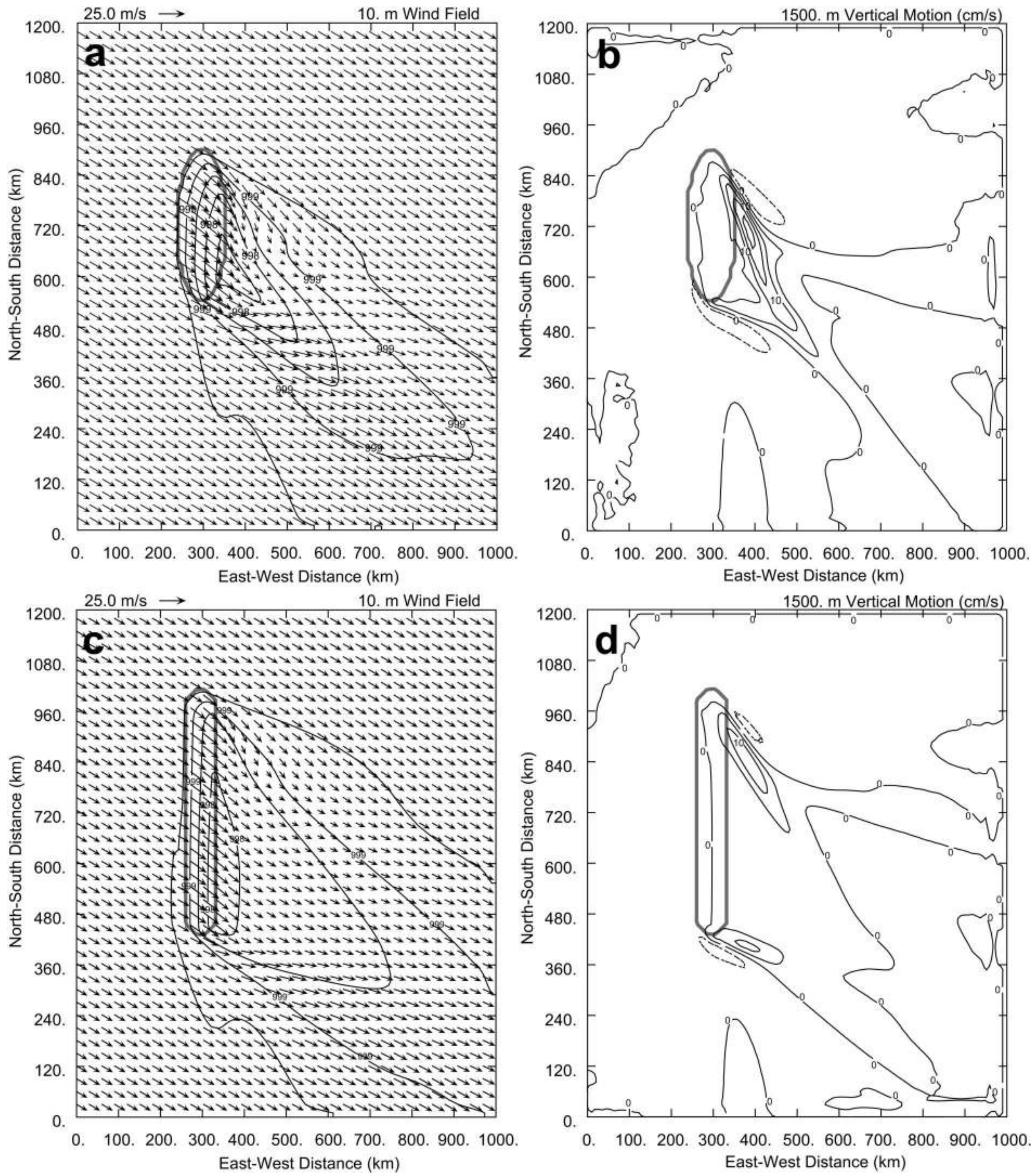

FIG. 3. Same as Fig. 1, but with an ambient wind speed of 18.2 m s^{-1}.

2a,b show that a strong shoreline band develops along a large extent of the eastern lake shoreline and curves inland near the southeastern shore. The corresponding simulation with a circular lake and equivalent *U*, ΔT, and *N* (Figs. 3c,d of Laird et al. 2003) produced a shoreline band with similar structure but greater maximum updraft. The weaker overlake acceleration of the winds resulting from the reduced fetch in the 3:1 simulation produced weaker near-surface frictional convergence at the downwind shore and a reduction in the updraft of the shoreline band. For example, the maximum vertical motion decreased from 47.7 to 32.1 cm s^{-1} for the circular-lake and northwest 3:1 simulations, respectively.

The shoreline band that developed from 10 m s^{-1} flow over the 3:1 elliptical lake (Figs. 2a,b) differed significantly from the results of prior studies. Hsu (1987) found that two updraft regions developed when using both linear and nonlinear mesoscale models to simulate a moderate LE event (i.e., maximum $\Delta\theta = 10$ K), with northwest wind speeds of 10 m s^{-1} over Lake Michigan (approximate 3:1 axis ratio). One region was positioned along the northeastern shoreline near Traverse City, Michigan, and the other region was located to the south near Benton Harbor, Michigan. Both of the updraft regions simulated by Hsu (1987) extended from near the downwind shoreline for more than 100 km inland (Fig. 23 of Hsu 1987).

The results shown in Figs. 2c,d differ greatly from the simulations with 3:1 elliptical and circular lakes and are similar to findings from Hsu (1987) for northwest flow of 10 m s^{-1}. The change from a 3:1 to 9:1 lake axis ratio resulted in a transition from a single shoreline band along the downwind lakeshore to the development of two updraft regions near the downwind shore. Figures 2c,d show a shoreline band along the northern section of the downwind shore, a transition to widespread coverage along the southern portion of the downwind shoreline, and an enhanced updraft region associated with a lake-end convergence zone extending inland from the southeastern lakeshore. This lake-end convergence zone is similar to a feature observed by Baker (1976) and simulated by Rose (2000) at the southern end of Lake Michigan.

The location of the shoreline bands in Fig. 2 is directly linked to the position and strength of the mesolow that developed as a result of the interaction of the ambient flow and the surface sensible heating from the lake. In both simulations, the mesolow is located along the southeast shoreline. In the 9:1 simulation, the mesolow is weaker and more elongated in the north–south direction. These two characteristics result in a weaker land breeze restricted to the northern half of the downwind shoreline. While both updraft regions simulated by Hsu (1987) extended downwind of the lake, only the southern updraft in the 9:1 simulation was similar in orientation to the prevailing wind. The northern updraft region was parallel to the downwind shore (i.e., shoreline band) because of the land breeze in this region. The restriction of the land breeze to northern portions of the lake also resulted in the low-level convergence zone and vertical motions for the northern maximum being stronger than the southern maximum. This difference likely resulted from the use of a larger ΔT (i.e., 22.5°C) than used by Hsu (1987) and indicates that ΔT likely plays a role in the position, orientation, and intensity of LE convergence zones. Although the morphology of LE mesoscale circulations was not found by Laird et al. (2003) to be dependent on ΔT, during shoreline band simulations over circular and elliptical lakes, the band position and intensity was dependent on the magnitude of ΔT.

3) 18.2 M S^{-1} NORTHWEST WIND SIMULATIONS

The structure of the mesoscale circulations from the 18.2 m s^{-1} northwest wind 3:1 and 9:1 lake axis ratio simulations shown in Fig. 3 have similar features to the LE circulations from the 10.0 m s^{-1} simulations (Fig. 2). The primary difference between the 10.0 and 18.2 m s^{-1} simulations is that a localized land breeze developed along the downwind shoreline in the 10.0 m s^{-1} simulations and not in the 18.2 m s^{-1} simulations. In the 3:1 lake axis ratio simulation (Figs. 3a,b), a coherent mesoscale band extended inland from the northern downwind shore at an angle of approximately 35° to the ambient wind direction. Technically, this simulation yields a widespread morphology by our definition because of the lack of a land-breeze circulation. However, the presence of the *strong coherent* band at the northern end of the lake suggests that the 3:1 lake axis ratio simulation should be classified as an LE morphology comprising both widespread coverage and shoreline band structural characteristics. The presence of similar prominent LE structures in several of the elliptical-lake simulations seems to indicate that the morphological transition zones in U/L parameter space may be wider than suggested by the results from the circular-lake simulations by Laird et al. (2003).

The fields shown in Figs. 3c,d for the 9:1 simulation are very similar to those shown by Hsu (1987), with two weak updraft regions at the northern and southern ends of the lake embedded within a large area of widespread weaker updraft. The enhanced regions are associated with weak low-level convergence zones located downwind of the lake, extending inland with an orientation closer to the prevailing wind. The mesolow positioned near the downwind shore is weak and elongated along the eastern shoreline of the 9:1 lake.

b. Mesoscale morphology sensitivity to U/L

Figure 4 presents the relationships of U/L to the morphology of the LE mesoscale circulation from each of the simulations with an elliptical lake and maximum vertical motion. Circular-lake results from Laird et al. (2003) for wind speeds of 1.0, 10.0, and 18.2 m s^{-1} are provided for direct comparison with the elliptical-lake results. The lake axis ratio, wind direction, and wind speed information is included in Fig. 4. For example, simulations having a northwest wind and 9:1 lake axis ratio are denoted by the abbreviation nw9 and a small open triangle. The simulations with a circular lake are designated using an asterisk.

The morphology of the LE circulation that developed in each simulation is indicated by large blue circles, yellow triangles, and green squares for a vortex, shoreline band, or widespread coverage morphology, respectively. When two overlapping shapes are used, the simulated mesoscale structure exhibited a combination of two LE morphologies. For example, the LE circulation from the nw9 simulation with winds of 10 m s^{-1} (Figs. 2c,d) exhibited characteristics of both a shoreline band and widespread coverage morphology over different areas near the downwind shoreline. In the vicinity of the

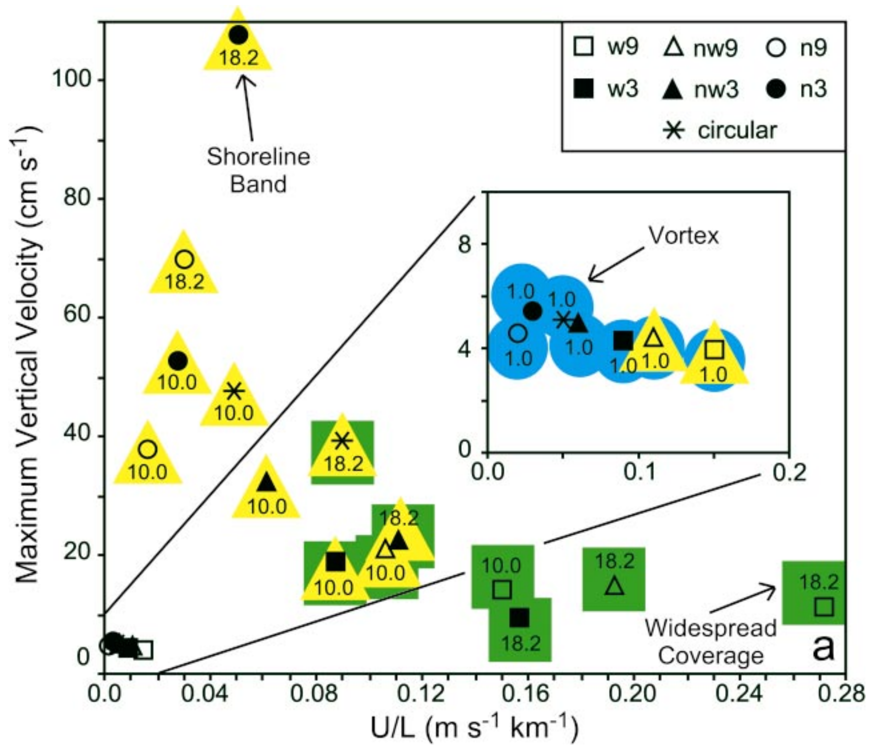

FIG. 4. The ratio of wind speed to maximum fetch distance (U/L) vs maximum vertical motion for the series of 21 simulations. Large blue circles, yellow triangles, and green squares denote mesoscale vortex, shoreline band, and widespread coverage LE morphologies, respectively. Labels represent ambient wind speed (m s^{-1}). Wind direction and lake axis ratio are identified by small symbols in the legend (e.g., nw9 identifies the simulation with a northwest wind and 9:1 lake axis ratio). Asterisks represent circular lake simulations. Inset shows enlarged low-U/L region.

northern downwind shore, a localized land breeze existed, resulting in the development of a weak shoreline band. Over the southern downwind shore, nearly unidirectional winds resulted in a diffuse region of weak vertical motions (i.e., widespread coverage morphology).

For a given lake axis ratio and wind speed, the change from northerly winds (small circles) to northwesterly winds (small triangles) and then to westerly winds (small squares) resulted in a significant shift of mesoscale structure from shoreline band toward widespread coverage morphologies for wind speeds of 10.0 and 18.2 m s^{-1}. For simulations with wind speeds of 1.0 m s^{-1}, the same change in wind direction resulted in a minor shift of the morphology from vortex toward shoreline band; however, the 3:1 lake axis ratio simulations with wind speeds of 1.0 m s^{-1} produced a vortex circulation for each wind direction. The shift in LE morphology from vortex toward shoreline band and from shoreline band toward widespread coverage with a change of wind direction from northerly toward westerly corresponds to a reduction of the maximum fetch distance and an increase in U/L. This finding is consistent with observations of LE shoreline band and widespread coverage events over Lakes Erie, Ontario, and Michigan, with changes of wind direction from along to across a lake's major axis. For example, Lake Michigan shoreline bands typically occur under northerly wind conditions, when the fetch distance is greatest and the east–west wind component is smallest (e.g., Passarelli and Braham 1981; Hjelmfelt 1990). Alternatively, Lake Michigan widespread coverage events generally form with northwest or west winds (e.g., Kristovich and Laird 1998), and Lake Michigan vortex events most frequently occur under weak wind conditions with a preferred northerly wind direction (e.g., Forbes and Merritt 1984; Hjelmfelt 1990).

Results from the current study demonstrate that U/L remained a valuable parameter for determining the structure of an LE circulation, even when variations of lake shape, wind direction, and wind speed were introduced. Figure 4 shows that the simulated LE conditions with low U/L values (<0.02 m s^{-1} km^{-1}) resulted in a vortex circulation or a combined morphology with vortex and shoreline band. Conditions leading to intermediate values of U/L (0.02 to $\sim$0.09 m s^{-1} km^{-1}) tended to result in the development of a shoreline band (e.g., land-breeze convergence zone). A wide U/L morphological transition zone between shoreline bands and widespread coverage was found to exist near U/L = 0.09 m s^{-1} km^{-1}. Values of U/L greater than approximately 0.11 m s^{-1} km^{-1} produced widespread coverage within a region over and downwind of the lake.

4. Summary and conclusions

A series of mesoscale model simulations with an isolated elliptical lake and prescribed environmental conditions was used to examine the influences of lake shape, wind speed, and wind direction on the structure and intensity of LE circulations. The simulated fields often exhibited more complex structures than those produced in many of the simulations with circular lakes. In addition to the three primary LE morphologies (i.e., vortices, bands, and widespread coverage), several of the LE structures exhibited a mixture of two morphologies, with structural features of both often simultaneously located in different areas either over the lake, near the downwind shoreline, or inland from the downwind shore.

For a given lake axis ratio and ambient wind speed of 10.0 or 18.2 m s^{-1}, the change from winds along to across the major lake axis resulted in a significant shift of mesoscale morphology from shoreline band toward widespread coverage. For simulations with wind speeds of 1.0 m s^{-1} and a large axis ratio (i.e., 9:1), a change in winds from along to across the major lake axis resulted in a shift of morphology from vortex toward shoreline band. Weak winds across lakes with small axis ratios (i.e., 1:1 or 3:1) produced mesoscale vortices for each wind direction. In all cases, the shift in mesoscale LE morphology from vortices toward widespread coverage with a change of wind direction corresponded to a reduction of the maximum fetch distance and an increase in U/L.

As with circular lakes, the ratio of wind speed to maximum fetch distance was found to be a valuable parameter for determining the structure of a LE circulation even when variations of lake shape and wind direction were introduced. In addition, the transition between morphologies was gradual and occurred over a range of U/L values. This is similar to the result of Laird et al. (2003) for circular lakes that showed that the structure of the LE circulation within the U/L transition zones is an amalgamation of two morphologies and exhibits structural features of both, often in different areas over the lake, near the downwind shoreline, or inland from the downwind shore. However, the current results suggest that the U/L transition zones between LE morphologies may be wider because of the more complex lake shapes and the interaction of the ambient flow with the locally developed mesoscale circulations. The complex lake coastline configuration associated with several regions of the Great Lakes, the existence of local-scale LE circulations, such as ''enhanced'' bands (Holroyd 1971), and the interaction of meso-β- and meso-α-scale LE circulations (Mann et al. 2002) may further impact the actual width of the U/L morphological transitional zones for observed LE events.

APPENDIX

Simulations Conducted with Elliptical Lakes

TABLE A1. The initial lake–air temperature difference (ΔT = 22.5°C) and surface-to-1.5-km stability ($d\theta/dz$ = 1.0 K km^{-1}) were held constant for all simulations. Wind directions are north (N), northwest (NW), and west (W). Variables included in the table are wind speed (U), wind direction, maximum fetch distance (L), U/L, lake axis ratio, and lake-effect morphology [vortex (V), band (B), widespread (WS)]. The experiment numbers denoted with an asterisk (*) are simulations with circular lakes.

Experiment	U (m s^{-1})	Wind direction	L (km)	U/L (m s^{-1} km^{-1})	Lake axis ratio	Morphology
1	1.0	N	350.0	0.003	3:1	V
2	10.0	N	350.0	0.029	3:1	B
3	18.2	N	350.0	0.052	3:1	B
4	1.0	NW	161.0	0.006	3:1	V
5	10.0	NW	161.0	0.062	3:1	B
6	18.2	NW	161.0	0.113	3:1	B, WS
7	1.0	W	114.0	0.009	3:1	V
8	10.0	W	114.0	0.088	3:1	B, WS
9	18.2	W	114.0	0.160	3:1	WS
10	1.0	N	600.0	0.002	9:1	V
11	10.0	N	600.0	0.017	9:1	B
12	18.2	N	600.0	0.030	9:1	B
13	1.0	NW	93.0	0.011	9:1	V, B
14	10.0	NW	93.0	0.108	9:1	B, WS
15	18.2	NW	93.0	0.196	9:1	WS
16	1.0	W	66.0	0.015	9:1	V, B
17	10.0	W	66.0	0.152	9:1	WS
18	18.2	W	66.0	0.276	9:1	WS
19*	1.0	W	200.0	0.005	1:1	V
20*	10.0	W	200.0	0.050	1:1	B
21*	18.2	W	200.0	0.091	1:1	WS

Acknowledgments. The authors would like to extend thanks to Drs. Robert Rauber, Mohan Ramamurthy, Mark Hjelmfelt, and Peter Sousounis for their helpful suggestions and comments along the way to completion of this research. The National Science Foundation, through Grants ATM9816306 and ATM0202305, supported this research. Any opinions, findings, conclusions, or recommendations expressed in this material are those of the author(s) and do not necessarily reflect the views of the National Science Foundation.

REFERENCES

Baker, D. G., 1976: The mesoscale temperature and dew point fields of a very cold airflow across the Great Lakes. *Mon. Wea. Rev.,* **104,** 860–867.

Braham, R. R., Jr., 1983: The Midwest snow storm of 8–11 December 1977. *Mon. Wea. Rev.,* **111,** 253–272.

——, and R. D. Kelly, 1982: Lake-effect snow storms on Lake Michigan, USA. *Cloud Dynamics,* E. Agee and T. Asai, Eds., D. Reidel, 87–101.

Cooper, K. A., M. R. Hjelmfelt, R. G. Derickson, D. A. R. Kristovich, and N. F. Laird, 2000: Numerical simulation of transitions in boundary layer convective structures in a lake-effect snow event. *Mon. Wea. Rev.,* **128,** 3283–3295.

Forbes, G. S., and J. M. Merritt, 1984: Mesoscale vortices over the Great Lakes in wintertime. *Mon. Wea. Rev.,* **112,** 377–381.

Hjelmfelt, M. R., 1990: Numerical study of the influence of environmental conditions on lake-effect snowstorms on Lake Michigan. *Mon. Wea. Rev.,* **118,** 138–150.

——, and R. R. Braham Jr., 1983: Numerical simulation of the airflow over Lake Michigan for a major lake-effect snow event. *Mon. Wea. Rev.,* **111,** 205–219.

Holroyd, E. W., III, 1971: Lake-effect cloud bands as seen from weather satellites. *J. Atmos. Sci.,* **28,** 1165–1170.

Hsu, H.-M., 1987: Mesoscale lake-effect snowstorms in the vicinity of Lake Michigan: Linear theory and numerical simulations. *J. Atmos. Sci.,* **44,** 1019–1040.

Kelly, R. D., 1986: Mesoscale frequencies and seasonal snowfalls for different types of Lake Michigan snowstorms. *J. Climate Appl. Meteor.,* **25,** 308–321.

Kristovich, D. A. R., and N. F. Laird, 1998: Observations of widespread lake-effect cloudiness: Influences of lake surface temperature and upwind conditions. *Wea. Forecasting,* **13,** 811–821.

Laird, N. F., 1999: Observation of coexisting mesoscale lake-effect vortices over the western Great Lakes. *Mon. Wea. Rev.,* **127,** 1137–1141.

——, 2001: Simulations of winter mesoscale circulations associated with an isolated lake. Ph.D. dissertation, University of Illinois at Urbana–Champaign, 146 pp. [Available from University Microfilms Inc., P.O. Box 1346, Ann Arbor, MI 48106.]

——, D. A. R. Kristovich, and J. E. Walsh, 2003: Idealized model simulations examining the mesoscale structure of winter lake-effect circulations. *Mon. Wea. Rev.,* **131,** 206–221.

Lavoie, R. L., 1972: A mesoscale numerical model of lake-effect storms. *J. Atmos. Sci.,* **29,** 1025–1040.

Mann, G. E., R. B. Wagenmaker, and P. J. Sousounis, 2002: The influence of multiple lake interactions upon lake-effect storms. *Mon. Wea. Rev.,* **130,** 1510–1530.

McPherson, R. D., 1970: A numerical study of the effect of a coastal irregularity on the sea breeze. *J. Appl. Meteor.,* **9,** 767–777.

Niziol, T. A., 1987: Operational forecasting of lake effect snowfall in western and central New York. *Wea. Forecasting,* **2,** 310–321.

——, W. R. Snyder, and J. S. Waldstreicher, 1995: Winter weather forecasting throughout the eastern United States. Part IV: Lake effect snow. *Wea. Forecasting,* **10,** 61–77.

Passarelli, R. E., Jr., and R. R. Braham Jr., 1981: The role of the winter land breeze in the formation of Great Lake snow storms. *Bull. Amer. Meteor. Soc.,* **62,** 482–491.

Pease, S. R., W. A. Lyons, C. S. Keen, and M. R. Hjelmfelt, 1988: Mesoscale spiral vortex embedded within a Lake Michigan snow squall band: High resolution satellite observations and numerical model simulations. *Mon. Wea. Rev.,* **116,** 1374–1380.

Pielke, R. A., 1974: A three-dimensional numerical model of the sea breezes over south Florida. *Mon. Wea. Rev.,* **102,** 115–139.

Pitts, D. E., J. T. Lee, J. Fein, Y. Sasaki, K. Wagner, and R. Johnson, 1977: Mesoscale cloud features observed from Skylab. *Skylab Explores the Earth,* NASA-SP-80, Scientific and Technical Information Office, NASA, 479–501.

Rose, B. L., 2000: The role of upstream lakes in determining downstream severe lake-effect snowstorms. Ph.D. dissertation, University of Illinois at Urbana–Champaign, 183 pp. [Available from University Microfilms Inc., P.O. Box 1346, Ann Arbor, MI 48106.]

Rothrock, H. J., 1969: An aid in forecasting significant lake snows. NWS Tech. Memo. WBTM CR-30, NWS Central Region, Kansas City, MO, 12 pp.

Schoenberger, L. M., 1986: Mesoscale features of the Michigan land breeze using PAM II temperature data. *Wea. Forecasting,* **1,** 127–135.

Sousounis, P. J., 1993: A numerical investigation of wind speed effects on lake-effect storms. *Bound.-Layer Meteor.,* **64,** 261–290.